INDONESIAN JOURNAL OF LIFE SCIENCES

RESEARCH ARTICLE

Check for updates

OPEN ACCESS

Integrated Network Pharmacology and Molecular Docking Identify Neuroprotective Candidates from *Nicotiana tabacum* L. Against Alzheimer's Disease

Daffa' Rizal Dzulfaqaar Alauddin[1]*, Muhammad Januar Wicaksono[2], Muhammad Abas[2], Zubair Alkwarismi[2], Mochamad Abdillah Wasom[2], Rini Madyastuti Purwono[1]

[1]*Departement of Veterinary Biomedical Science, Sub Division of Veterinary Pharmacy, School of Veterinary Medicine and Biomedical Science, IPB University, Bogor, West Java, 16680, Indonesia*

[2]*Mathematics and Natural Sciences, SMA Islam HASMI, Bogor, West Java, 16600, Indonesia*

**Corresponding author: daffa.rizal@apps.ipb.ac.id*

ARTICLE INFO

Article history:

Submitted November 22, 2025
Revised February 9, 2026
Accepted February 10, 2026

DOI: 10.54250/ijls.v8i01.288

KEYWORDS:

Alzheimer's disease, Molecular docking, Network pharmacology, Neuroprotection, Nicotiana tabacum L.

HIGHLIGHTS

- IL-1β, GSK3β, and AChE were identified as central Alzheimer's targets from network analysis
- 28-Isofucosterol, β-amyrin, and Granisterol were balanced multi-target leads
- BOILED-Egg favored moderately lipophilic compounds with TPSA < 79 Å^2 for BBB-oriented prioritization

ABSTRACT

The neuroprotective potential of compounds from *Nicotiana tabacum* L. against Alzheimer's disease was evaluated using network pharmacology, molecular docking, and ADME profiling. 25 compounds were screened, and the intersection of predicted targets with Alzheimer's disease associated proteins yielded 90 overlapping proteins. Network topology using Degree prioritized three hub targets, IL-1β (Degree: 37), GSK3β (Degree: 25), and AChE (Degree: 19). Docking in YASARA against IL-1β (5R8Q), GSK3β (5K5N), and AChE (4EY7) produced binding energy ranges of -6.673 to -8.680, -9.769 to -10.614, and -10.349 to -12.275 kcal/mol, respectively. The β-amyrin ranked best among test ligands for IL-1β at -6.885 kcal/mol and for GSK3β at -10.178 kcal/mol, while citrostadienol ranked best for AChE at -10.881 kcal/mol. Dual-target profiles supported 28-Isofucosterol for GSK3β and AchE, and gramisterol for IL-1β and AChE. BOILED Egg analysis supported BBB-oriented prioritization of candidates with TPSA <79 Å², while highly lipophilic sterol-type leads indicate formulation-dependent developability. Overall, *Nicotiana tabacum* L. provides non-nicotine sterol and triterpenoid scaffolds as multi-target chemotypes spanning inflammation, kinase signaling, and cholinergic dysfunction in Alzheimer's disease.

INTRODUCTION

Alzheimer's disease (AD) is a progressive neurodegenerative disorder and the leading cause of dementia in older adults (Sayas & Ávila, 2021). Neuropathology is characterized by extracellular amyloid-β (Aβ) deposition and intracellular neurofibrillary tangles composed of hyperphosphorylated tau, accompanied by synaptic loss and widespread network dysfunction (Sayas & Ávila, 2021). While amyloid and tau remain central hallmarks, mounting evidence supports AD as a systems-level disorder in which neuroinflammation, kinase-driven tauopathy, and neurotransmitter failure reinforce one another across disease stages. Three biologically connected axes are especially relevant to this network behavior: chronic neuroinflammation centered on interleukin-1β (IL-1β), kinase-mediated tau pathology dominated by glycogen synthase kinase-3β (GSK3β), and cholinergic hypofunction represented by acetylcholinesterase (AChE) (Birks & Harvey, 2018; Li & Gong, 2025).

IL-1β is a key effector cytokine downstream of inflammasome signaling in microglia. Aβ species and damage-associated cues promote inflammasome activation and IL-1β maturation, sustaining a feed-forward inflammatory milieu that contributes to synaptic injury and neuronal vulnerability (Hanslik & Ulland, 2020; Li & Gong, 2025; McManus & Latz, 2024). GSK3β contributes to tau hyperphosphorylation at disease-relevant epitopes and biases neuronal survival pathways toward degeneration. Increased GSK3β signaling has been reported in AD brains and preclinical models (Lauretti et al., 2020). AChE represents a clinically validated symptomatic axis: inhibiting AChE elevates synaptic acetylcholine and can transiently improve cognition and function, although it does not halt neurodegeneration (Birks & Harvey, 2018; Marucci et al., 2021). Critically, these axes are mechanistically interlinked, which supports a rational multi-target inflammation, kinase, and cholinergic strategy rather than three independent targets.

Neuroinflammatory IL-1β signaling can exacerbate tau pathology by engaging stress-kinase cascades and has been linked to increased tau phosphorylation via pathways that include p38-MAPK and/or GSK3β in experimental AD contexts, providing a molecular bridge between cytokine tone and tau-kinase activity (Chen & Yu, 2023). Conversely, GSK3β serves as a convergence point for neuronal survival signaling, including PI3K and Akt mediated regulation of GSK3β activity, and for inflammatory responses, making it relevant not only to tau phosphorylation but also to neuroinflammation-associated signaling states in the Alzheimer's disease brain (Pan et al., 2024). The cholinergic axis interacts with inflammation through the cholinergic anti-inflammatory pathway, in which acetylcholine signaling can dampen pro-inflammatory cytokine release, including IL-1β, in immune cells and neuroimmune interfaces. Therefore, cholinergic hypofunction may remove an endogenous brake on inflammatory escalation, while AChE inhibition may provide symptomatic benefit and may also contribute to anti-inflammatory effects (Cantone et al., 2024). Together, these links justify pursuing coherent polypharmacology across IL-1β, GSK3β, and AChE as a more comprehensive therapeutic rationale than single-target screening.

Drug discovery in AD remains difficult because interacting pathways create redundancy, compensatory feedback, and stage-dependent biology, while the blood-brain barrier (BBB) constrains pharmacology. Network pharmacology can address this complexity by integrating compound–target–pathway relationships at a systems level to highlight mechanism coherence and identify central nodes for intervention (Li et al., 2021). When coupled with molecular docking, structure-guided prioritization becomes possible within selected hubs, improving the likelihood of identifying candidates with plausible binding at multiple disease-relevant proteins (Pinzi & Rastelli, 2019). *Nicotiana tabacum* L. is often discussed primarily for nicotine and tobacco-related health burdens. However, the plant also contains diverse non-nicotine secondary metabolites, including sterols, terpenoids, and polyphenols, with reported bioactivities in antioxidant, anti-inflammatory, and neuroactive domains (Wu et al., 2025; Zhang et al.,

2024). Importantly, what remains insufficiently characterized is a target-guided and system-level mapping of *N. tabacum* L. metabolites beyond nicotine against an integrated Alzheimer's disease triad that links neuroinflammation, tau kinase signaling, and cholinergic dysfunction. In particular, prior discussions of *N. tabacum* L. phytochemicals have not consistently integrated network-based hub nomination, structure-based docking at the nominated hubs, and early ADME and brain access triage to produce a concise shortlist grounded in mechanism.

This study applies an integrated network pharmacology and molecular docking strategy to identify *N. tabacum* L. derived neuroprotective candidates against AD, with an a priori emphasis on IL-1β, GSK3β, and AChE as a mechanistically connected triad. The workflow compiles *N. tabacum* L. phytochemicals from curated sources, infers putative AD-relevant targets through network analysis and pathway enrichment, and conducts structure-based docking to rank ligands by binding plausibility at the three axes. The objective is to generate a concise shortlist of non-nicotine-enriched chemotypes with a coherent multi-pathway rationale for subsequent experimental validation.

MATERIALS AND METHODS

Materials

This study utilized several curated databases and specialized software. Bioactive phytochemicals were retrieved from TCMSP v3.0, ETCM v2.0, IMPPAT v2.0, and KNApSAcK Family (accessed in September 2025). Target prediction and annotation were conducted using SwissTargetPrediction, UniProt, GeneCards v5.26.0, and DrugBank v5.1.14 (accessed in September 2025). Network construction was performed in Cytoscape v3.10.3 integrated with the CytoNCA and Cytohubba plugins. Gene Ontology (GO) enrichment analysis and Kyoto Encyclopedia of Genes and Genomes (KEGG) were performed using ShinyGO v0.85.1 for *Homo sapiens*. Molecular docking simulations were carried out using YASARA Structure v19.9.17, with visualization generated via BIOVIA Discovery Studio Visualizer 2016 and PyMOL v3.1.5.1.

Methods

Screening strategy for bioactive compounds in *N. tabacum* L.

Bioactive constituents of *N. tabacum* L. were compiled from the aforementioned phytochemical databases. 3D Chemical structures and SMILES were retrieved from PubChem, and duplicates were removed based on InChIKey matching. To ensure therapeutic viability, a strict pharmacokinetic screening was applied using SwissADME. Compounds were retained only if they met the following criteria, including Lipinski's Rule-of-Five compliance (MW ≤ 500, LogP ≤ 5, H-donors ≤ 5, H-acceptors ≤ 10) and zero alerts in the PAINS (Pan-Assay Interference Compounds) filter. Only compounds satisfying these oral drug-likeness criteria were subjected to downstream target prediction.

Identification of Alzheimer's disease-associated targets

Molecular target prediction was performed using SwissTargetPrediction with *Homo sapiens* species; only targets with probability values ≤0.10 were retained and then limited to ≤100 top targets. All targets were then standardized for identity using UniProt. Alzheimer's disease targets were obtained from GeneCards using the keyword "Alzheimer's"; targets were then prioritized based on a relevance score ≥3. Compound targets and disease targets were then intersected to obtain overlapping targets used as candidates for anti-Alzheimer's mechanisms. Intersections were calculated using Venny v2.1.0.

Construction of active compound-target-pathway network

Overlapping targets were then entered into STRING v12.0 using the *Homo sapiens* organism to construct a protein-protein interaction network. Hub ranking was performed in cytoHubba using degree as the primary score and cross-checked using betweenness or closeness to ensure robustness of the nominated hubs. GO and KEGG enrichment analyses were performed using ShinyGO on *Homo sapiens* organisms by inputting a list of overlapping target genes. ShinyGO calculated significance using the hypergeometric test with a false discovery rate (FDR) parameter of ≤0.05 and a fold enrichment of ≥1.5. In addition, to avoid bias, GO and KEGG analyses were run using pathway sizes of ≥10 and ≤500.

Molecular docking

Molecular docking was performed using YASARA Structure v19.9.17. Docking was conducted against three human Alzheimer's disease-related proteins: interleukin-1β (PDB ID: 5R8Q), glycogen synthase kinase-3β (PDB ID: 5K5N), and acetylcholinesterase (PDB ID: 4EY7), retrieved from the RCSB Protein Data Bank. All receptor structures originated from *Homo sapiens* and were solved as protein–ligand complexes at crystallographic resolutions of 1.23 Å (5R8Q), 2.20 Å (5K5N), and 2.35 Å (4EY7). Accordingly, the receptors used in this study were defined as the human forms of IL-1β, GSK3β, and AChE, as indicated by their UniProt accessions P01584, P49841, and P22303. Receptor preparation was performed in YASARA by selecting the relevant monomeric chain, removing crystallographic water molecules and non-essential heteroatoms, adding hydrogen atoms, and assigning protonation states under physiological conditions. The co-crystallized ligands present in each PDB complex were treated as native reference ligands for docking protocol validation via redocking. The protocol was considered valid when the redocked pose reproduced the experimental binding mode with RMSD ≤ 2.0 Å. Docking grids were centered on the native ligand-binding pocket and defined using the following grid center coordinates (x, y, z; Å): (14.19, 14.19, 14.19) for 5R8Q, (29.59, 29.59, 29.59) for 5K5N, and (23.15, 23.15, 23.15) for 4EY7. Grid-box boundaries were expanded from the binding-site limits using a target-specific grid-box padding of 2 Å (5R8Q), 9 Å (5K5N), and 4 Å (4EY7) to ensure that key pocket residues and surrounding interaction regions were fully captured.

Docking was executed using the AutoDock Vina engine implemented in YASARA with the following search parameters: exhaustiveness = 8, num_modes = 10, and energy_range = 3 kcal/mol. To address stochastic variability, each ligand–protein docking was repeated three times using different random seeds. For reporting, the best-scoring pose (lowest ΔG) across the three runs was used for ranking, while reproducibility was assessed by confirming consistent pocket localization and comparable pose orientation across replicates. Docking outputs included the predicted Gibbs free energy of binding (ΔG, kcal/mol) and the corresponding inhibition constant. Binding affinity was interpreted based on the principle that more negative ΔG values and lower inhibition constant values indicate stronger ligand–protein interactions. Three-dimensional visualization of protein–ligand complexes was performed using PyMOL v3.1.5.1, and two-dimensional interaction diagrams were generated using BIOVIA Discovery Studio Visualizer 2016.

RESULTS

Physicochemical properties

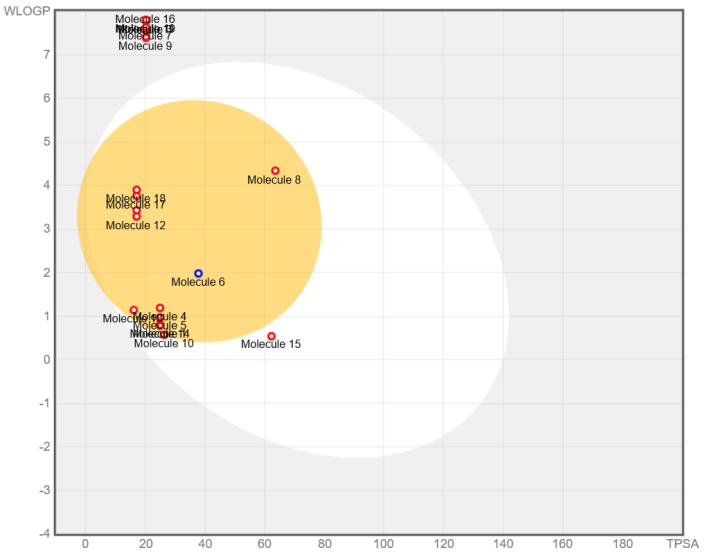

Figure 1. ADME profile based on BOILED-Egg

The SwissADME BOILED Egg plot uses WLOGP and TPSA to estimate passive gastrointestinal absorption and passive blood-brain barrier (BBB) permeation. In this model, the BBB permeation region is typically associated with TPSA < 79 Å² and WLOGP between 0.4 and 6.0, while the high intestinal absorption region is typically associated with TPSA below 142 Å² and WLOGP between -2.3 and 6.8. **Figure 1** shows that 13 of 20 *N. tabacum* L. constituents fall within the BBB permeation space and also within the intestinal absorption space, with TPSA values from 16.13 to 63.60 Å² and WLOGP values from 0.54 to 4.34. The remaining 7 of 20 compounds fall outside the BOILED Egg absorption windows because of very high lipophilicity, with WLOGP from 7.39 to 8.02, despite low TPSA near 20.23 Å², namely 24-methylenecholesterol, 31-norcycloartenol, campesterol, cholesterol, Granisterol, sitosterol, and stigmasterol. Anatalline is predicted as a P-glycoprotein substrate, which may reduce net brain exposure through efflux. Therefore, CNS-oriented prioritization favors BBB space compounds that are non-substrates of P-glycoprotein and show balanced polarity and lipophilicity, while sterol and triterpenoid candidates should be handled under a formulation plan or treated as peripheral comparators because their WLOGP values place them outside the model domain.

Table 1. ADMET profile and druglikeness of compounds in *Nicotiana tabacum* L.

Ligands	TPSA*	WLOGP*	MW*	HBD*	HBA*	Lipinski Violations	PAINS #Alerts*
(R)-(+)-nornicotine	24.92	0.8	148.2	1	2	0	0
24-methylenecholesterol	20.23	7.55	398.67	1	1	0	0
28-isofucosterol	20.2	8.52	412.69	1	1	0	0
31-norcycloartenol	20.23	7.78	412.69	1	1	0	0
Anabasine	24.92	1.19	162.23	1	2	0	0

Ligands	TPSA*	WLOGP*	MW*	HBD*	HBA*	Lipinski Violations	PAINS #Alerts*
Anatabine	24.92	0.97	160.22	0	2	0	0
Anatalline	37.81	1.98	239.32	1	3	0	0
β-amyrin	20.2	8.17	426.72	1	1	0	0
β-damascenone	17.07	3.43	190.29	0	1	0	0
Campesterol	20.23	7.63	400.68	1	1	0	0
Cembratrienediols	63.6	4.34	330.42	1	4	0	0
Cholesterol	20.23	7.39	386.65	1	1	0	0
Citrostadienol	20.2	8.19	426.72	1	1	0	0
Ethyl acetate	26.3	0.57	88.11	0	2	0	0
Granisterol	20.23	7.8	412.69	1	1	0	0
Megastigmatrienone D	17.07	3.29	192.27	0	1	0	0
Methylene-cholest-7-enol	20.2	8.47	386.65	1	1	0	0
Nicotine	16.13	1.14	162.23	0	2	0	0
Nornicotine	24.92	0.8	148.2	1	2	0	0
Obtusifoliol	20.2	8.34	426.72	1	1	0	0
Scopolamine	62.3	0.54	303.35	1	6	0	0
Sitosterol	20.23	8.02	414.71	1	1	0	0
Solanone	17.07	3.76	194.3	0	1	0	0
Solavetivone	17.07	3.9	218.33	0	1	0	0
Stigmasterol	20.23	7.8	412.69	1	1	0	0

*TPSA= Topological Polar Surface Area (Å^2); WLOGP= Wildman-Crippen LogP; MW= Molecular Weight; HBD= Hydrogen Bond Donor; HBA= Hydrogen Bond Acceptor; and PAINS= Pan-assay interference compounds.

Table 1 summarizes the ADMET profile and druglikeness of the 25 *Nicotiana tabacum* L. compounds and separates them into two physicochemical groups. Twenty-five compounds show TPSA values from 16.13 to 63.60 Å², WLOGP values from 0.54 to 4.34, and molecular weights from 88.11 to 426.72 Da. Seven compounds form a highly lipophilic sterol and triterpenoid group, namely 24-methylenecholesterol, 31-norcycloartenol, campesterol, cholesterol, Granisterol, sitosterol, and stigmasterol, with TPSA of 20.23 Å², molecular weights from 386.65 to 414.71 Da, and WLOGP values from 7.39 to 8.02, which indicates

higher solubility risk and formulation dependence even when PAINS alerts are zero and rule based filters are satisfied.

The intersected targets of *N. tabacum* L. and Alzheimer's disease

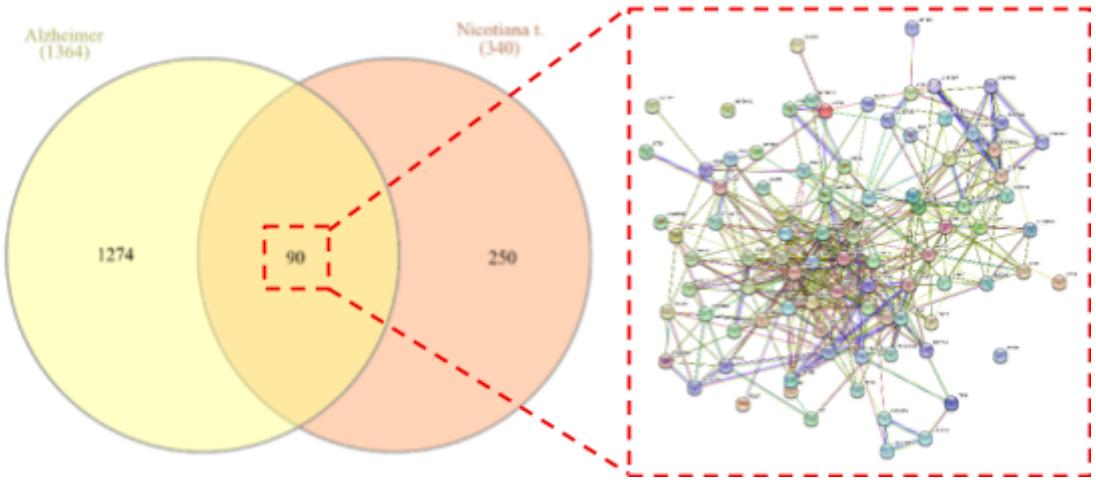

Figure 2. Target protein from intersection analysis of *N. tabacum* L. compounds and target protein of AD

Figure 2 shows the target proteins obtained from the intersection analysis between *N. tabacum* L. compound targets and Alzheimer's disease associated target proteins. From the union of predicted protein targets of *N. tabacum* L. bioactives and AD-associated proteins with high GeneCards relevance scores, intersection analysis yielded 90 overlapping proteins. This overlap indicates a biologically meaningful convergence between *N. tabacum* L. phytochemical activity and AD-relevant pathways, with IL-1β, GSK3β, and AChE emerging among the prioritized nodes for downstream validation.

GO and KEGG pathway enrichment analysis

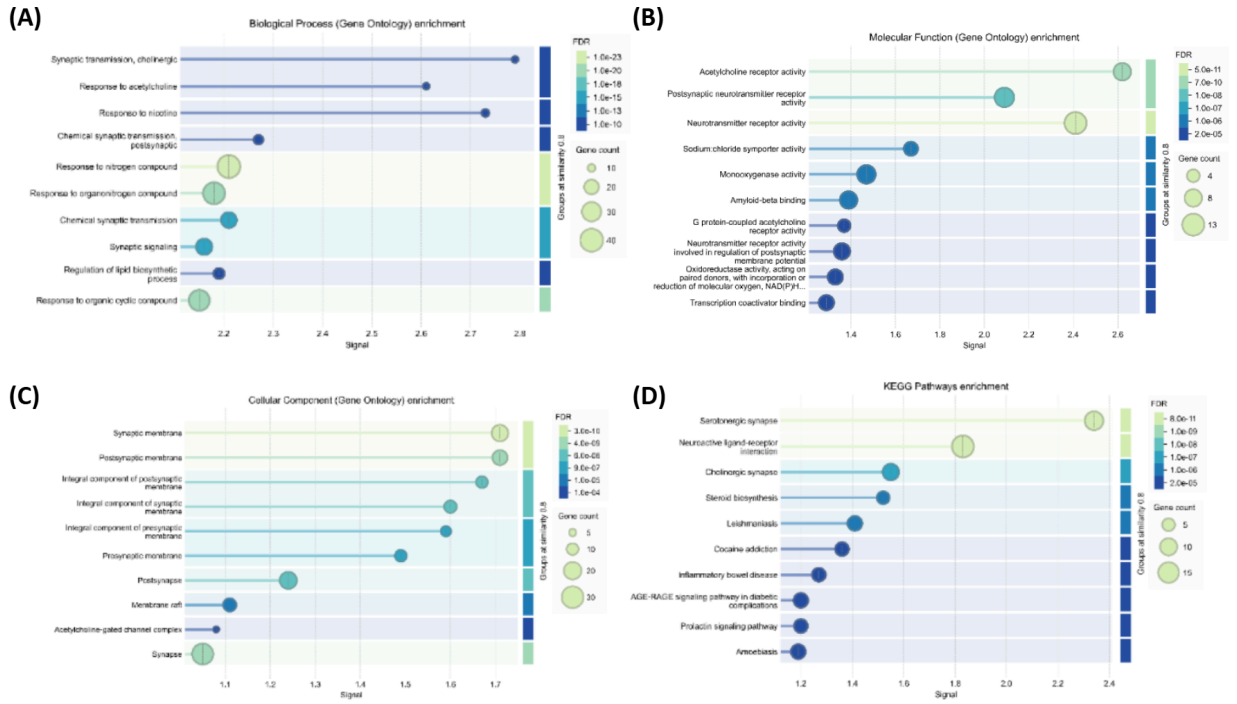

Figure 3. Gene Ontology (GO) categories (A) Biological Process, (B) Molecular Function, (C) Cellular Component, and (D) Kyoto Encyclopedia of Genes and Genomes (KEGG) pathways

Figure 3 presents the GO categories, including Biological Process, Molecular Function, and Cellular Component, together with Kyoto Encyclopedia of Genes and Genomes pathway enrichment for the 90 overlapping proteins. GO Biological Process terms were enriched for synaptic transmission, cholinergic signaling, response to acetylcholine, and response to nicotine, reflecting the cholinergic and nicotinic receptor pharmacology that is characteristic of *N. tabacum* L. alkaloids. GO Molecular Function highlighted acetylcholine receptor activity, neurotransmitter receptor activity, and postsynaptic neurotransmitter receptor activity. GO Cellular Component pointed to synaptic membrane, postsynaptic membrane, and presynaptic membrane, which is consistent with target localization at synapses that are affected early in Alzheimer's disease. KEGG pathway analysis implicated serotonergic synapse, neuroactive ligand receptor interaction, and cholinergic synapse, supporting a mechanistic link to neurotransmission, memory circuits, and neuroplasticity domains that intersect with Alzheimer's disease pathophysiology.

Screening *N. tabacum* L.-anti-Alzheimer's disease key targets and target interaction network

Table 2 reports the key nodes in the regulatory network of Alzheimer's disease target proteins ranked using the topological parameters Degree, Eigenvector, LAC, Betweenness, Closeness, and Network score. Network analysis identifies three principal nodes. IL-1β is the most central pro-inflammatory hub, GSK3β links tau hyperphosphorylation with neuronal survival pathways, and AChE functions as a specialized node within cholinergic regulation. These roles support prioritizing IL-1β and GSK3β as disease-modifying targets while AChE is retained as a validated symptomatic target, yielding a focused panel for structure-guided screening and docking of *N. tabacum* L. ligands.

Table 2. Nodes in the regulatory network of Alzheimer's disease target proteins based on topological parameters of Degree, Eigenvector, LAC (Local Average Connectivity), Betweenness, Closeness, and Network

Protein	*Degree*	*Eigenvector*	LAC	*Betweenness*	*Closeness*	*Network*
IL-1β	37	0.30530852	9.513514	1058.7211	0.27554178	26.713303
GSK3β	25	0.23895441	9.28	538.91125	0.26488096	15.25858
AChE	19	0.12099329	5.1578946	513.74084	0.25070423	9.291324

Analysis of core targets

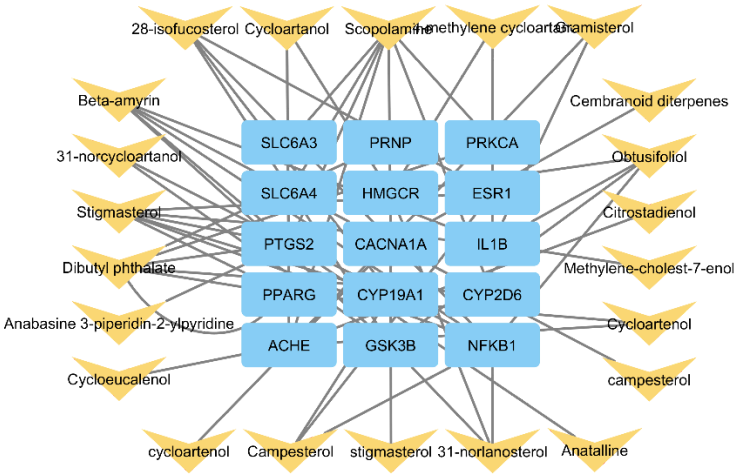

Figure 4. Composition of *N. tabacum* L. compounds with Alzheimer's disease target proteins

Figure 4 shows the composition of *N. tabacum* L. compounds with Alzheimer's disease target proteins in the integrated compound to target network. Network-level and literature anchored interpretation positioned IL-1β as a pivotal cytokine that propagates inflammatory signaling and contributes to synaptic dysfunction and neuronal injury in Alzheimer's disease contexts. GSK3β was linked to tau phosphorylation and neuronal transport defects, providing a route toward disease modification through kinase inhibition. AChE, although more modest in network degree than IL-1β and GSK3β, retained high clinical salience due to its role in cholinergic deficits and its successful pharmacological inhibition in current Alzheimer's disease care. These three proteins, therefore, constitute the core target triad for subsequent docking and ranking of *N. tabacum* L. molecules.

Molecular docking

Table 3. Amino acid residues of *N. tabacum* L. involved in molecular docking with target protein

Target	Ligands	Residues Involved in Molecular Docking	
		Hydrophobic Interactions	***Hydrogen Bonds***
IL-1β 5R8Q*	JGY	Leu69 **Pro131 Thr79** Phe134 Lys77 Pro78 **Gln81 Leu82**	**Val132 (4.02 Å)**, **Leu80 (3.77 Å)**, Leu26 (4.37 Å), Leu134 (4.53 Å), Tyr24 (6.14 Å), Glu25 (4.07 Å)
	β-amyrin	Pro78 **Thr79** Phe133 Lys77 Lys74 Tyr24 Gly22 Glu25 Pro23 Leu26 Pro131 **Val132** Leu80 **Gln81**	Leu134 (4.79 Å)
	Methylene-cholest -7-enol	**Leu82 Gln81** Glu25 Tyr24 Leu69 **Pro131 Thr79** Phe134 Leu134 Pro78 Lys77	**Leu80 (4.77 Å)**, Leu26 (4.37 Å)
	Granisterol	Tyr24 Pro23 Gly22 Glu25 **Pro131** Leu26 **Val132** Phe133 Lys77 Leu134 Pro78 Trp120 **Thr79 Leu80** Lys74 **Gln81**	-
GSK3β 5K5N*	PF-367	Met101 Phe201 Leu130 **Glu97** Ala83 Leu188 Ile62 Tyr134 Thr138 Gly62 Gln185 Val70 Gly65 Cys199 Phe67 **Asn186** Val110 **Asp200** Leu132 Lys85	Asn 64 (5.20 Å), Val135 (4.24 Å)
	β-amyrin	Arg141 Tyr140 Gln185 Thr138 **Asn186 Asp200** Leu188 Phe67 Cys199 Val110 Leu132 **Lys85** Ala83 Val70 Asn64 Gly63 Ile62	-
	28-isofucosterol	Leu132 Cys199 **Asp200 Asn186 Lys85** Gln185 Lys183 Asn64 Phe67 Gly63 Gly65 Val70 Thr138 Ile62 Arg141 Pro136 Glu137 Tyr134 Val135 Ala83 Leu188	-

Target	Ligands	Residues Involved in Molecular Docking	
		Hydrophobic Interactions	***Hydrogen Bonds***
	Obtusifoliol	Arg141 Tyr140 Gln185 Gly63 Thr138 Leu188 Val135 Ile62 Tyr134 Ala83 Val110 **Lys85** Val70 Cys199 **Asp200** Leu132 Phe201 **Asn186** Phe67 Lys183 Asn64 Gly65	-
AChE 4EY7*	Donepezil	Ser292 Leu289 Val294 Arg296 Tyr341 **Phe338** Gly448 Ile451 **Glu202 Tyr133** Gly120 **His447** Gly121 **Trp86 Tyr337** Asp74 Tyr124 Phe297 Trp286	Phe295 (5.12 Å), Tyr72 (5.85 Å), **Ser203 (4.01 Å)**
	Citrostadienol	Trp286 Asp74 Thr83 Gly448 **Trp86** Ser125 Gly121 Gly126 **Ser203** Ala204 Gly122 **Glu202 Tyr133 His447** Gly120 Ile451 **Tyr337 Phe338** Tyr341 Phe295 Tyr124 Arg296 Phe297 Val294 Ser293 Tyr72	-
	Granisterol	Ser125 Gly121 **Tyr133** Gly126 Gly120 Leu130 Gly122 **Ser203** Gly448 **Glu202** Hyr83 Asp74 Tyr341 Trp286 Tyr72 Phe297 Val294 Arg296 Tyr124 Ser293 Phe295 **Phe338 Tyr337 Trp86** His447	-
	28-isofucosterol	Ser293 Val294 Trp286 Tyr72 Asp74 Tyr124 **Trp86** Gly448 Ser125 Gly120 **Tyr133** Gly121 Gly126 **His447** Leu130 Gly122 Ser203 **Tyr337** Arg296 **Phe338** Phe342 Gly342 Ser293	Tyr341 (4.65 Å)

*PDB Identifiers

Bold = Catalytic Active Site (CAS) residue

Docking controls were confirmed and support the screening pipeline since donepezil ranked highest on AChE with ΔG -12.275 kcal/mol and Inhibition Constant 0.001 µM, PF367 ranked highest on GSK3β with ΔG -10.614 kcal/mol and Inhibition Constant 0.017 µM, and JGY ranked highest on IL-1β with ΔG -8.68 kcal/mol and Inhibition Constant 0.434 µM. **Table 4** shows that several *N. tabacum* L. metabolites approached these reference baselines on AChE and GSK3β, while binding on IL-1β was weaker yet reproducible. On AChE, citrostadienol achieved ΔG -10.881 kcal/mol with Inhibition Constant 0.011 µM, granisterol achieved ΔG -10.824 kcal/mol with Inhibition Constant 0.012 µM, and 28-isofucosterol achieved ΔG -10.349 kcal/mol with Inhibition Constant 0.026 µM. On GSK3β, β-amyrin achieved ΔG -10.178 kcal/mol with Inhibition Constant 0.035 µM, and 28-isofucosterol achieved ΔG -9.822 kcal/mol with Ki of 0.063 µM. On IL-1β, β-amyrin achieved ΔG -6.885 kcal/mol with Inhibition Constant 8.98 µM, while methylene-cholest-7-enol and granisterol showed similar ΔG values near -6.67 kcal/mol with Inhibition Constant near 12.8 µM.

Table 3 supports these rankings by showing consistent residue fingerprints across targets. On AChE, sterol ligands occupied the aromatic gorge and involved Trp86, Tyr337, Phe338, Tyr133, and Ser203, which aligns with the residue environment associated with effective cholinesterase inhibition. On GSK3β, β-amyrin and 28-isofucosterol contacted Lys85, Asp200, Cys199, Glu97, Asn186, and Val135 within the ATP pocket, mirroring the PF-367 binding environment and supporting a kinase inhibition rationale relevant to tau

phosphorylation. On IL-1β, granisterol, methylene-cholest-7-enol, and β-amyrin engaged a recurring hydrophobic patch involving Pro131 and Val132 with supportive contacts to Leu80 and Leu26. **Figures 5-7** visualize these interaction patterns by comparing each natural ligand with the best-ranked test ligand on the same target, which helps confirm that the top poses occupy the expected binding pockets and reproduce key active site contacts. Taken together, the residue fingerprints in **Table 3** and the affinity ranks in **Table 4** indicate a coherent polypharmacology profile. The 28-isofucosterol and granisterol present balanced multi-target behavior across AChE and GSK3β, with measurable binding on IL-1β, β-amyrin is prioritized for GSK3β, and citrostadienol is retained as an AChE-focused adjunct for symptomatic relevance.

Table 4. Gibbs free energy (ΔG) and inhibition constant values from molecular docking of *Nicotiana tabacum* L. test ligands against IL-1β, GSK3β, and ACHE target proteins

Target	Ligands	Gibbs free energy (kcal/mol)	Inhibition Constant (μM)
IL-1β	JGY	-8.68	0.434
	β-amyrin	-6.885	8.98
	Methylene-cholest-7-enol	-6.676	12.778
	Granisterol	-6.673	12.843
GSK3β	PF-367	-10.614	0.017
	β-amyrin	-10.178	0.035
	28-isofucosterol	-9.822	0.063
	Obtusifoliol	-9.769	0.069
AChE	Donepezil	-12.275	0.001
	Citrostadienol	-10.881	0.011
	Granisterol	-10.824	0.012
	28-isofucosterol	-10.349	0.026

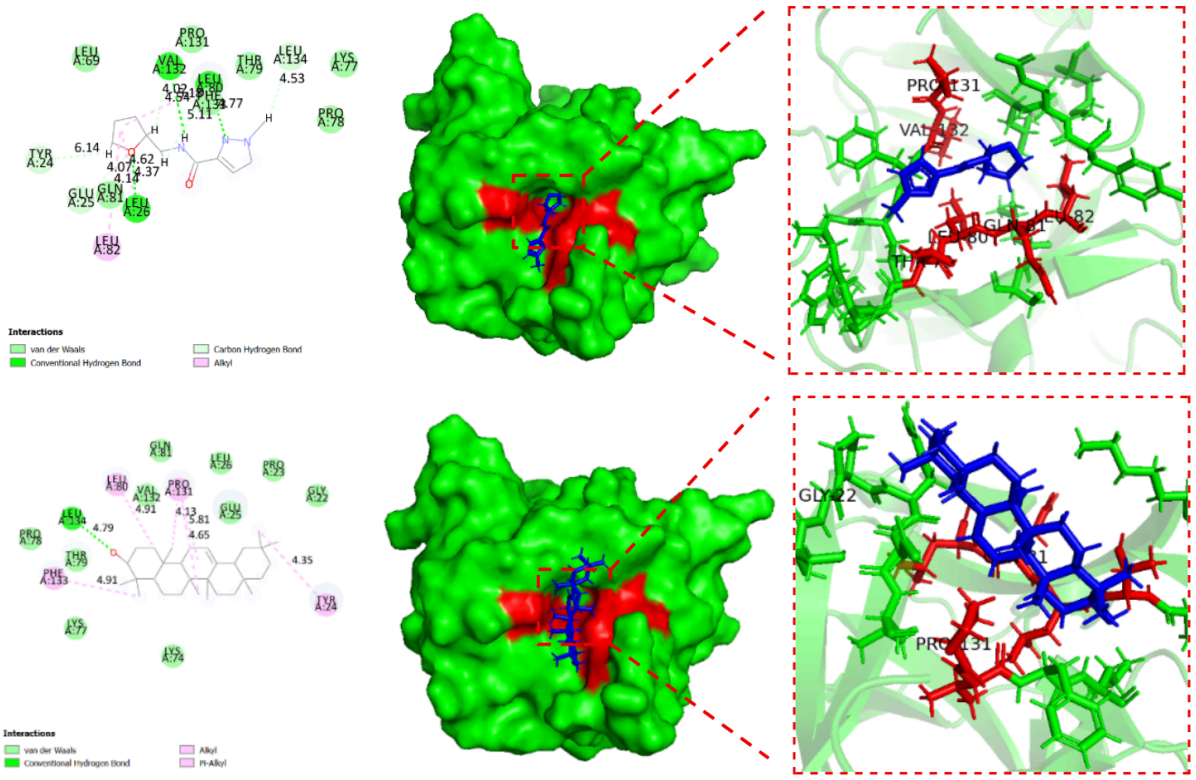

Figure 5. Visualization of 2D and 3D interactions between the natural ligand (JGY), the best test ligand (β-amyrin) based on Gibbs free energy (ΔG) values, and active residues of IL-1β protein

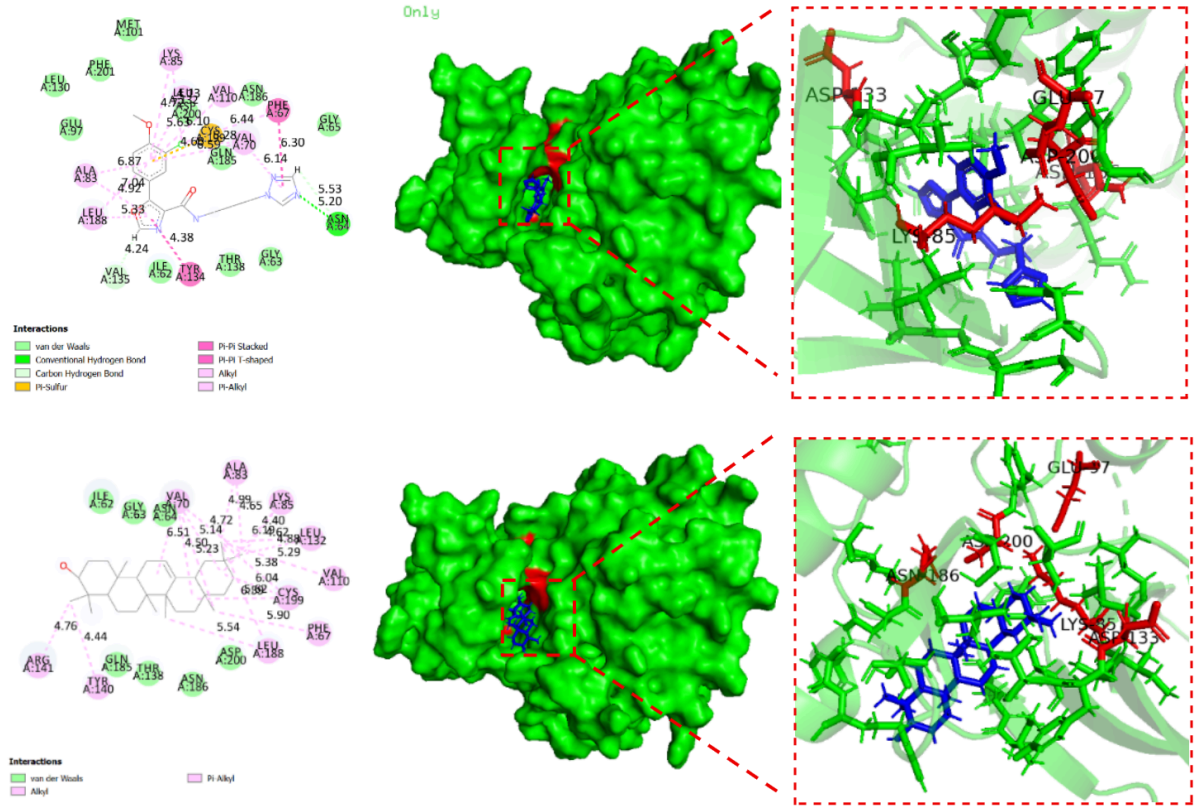

Figure 6. Visualization of 2D and 3D interactions between the natural ligand (PF-367), the best test ligand (β-amyrin) based on Gibbs free energy (ΔG) values, and active residues of GSK3β protein

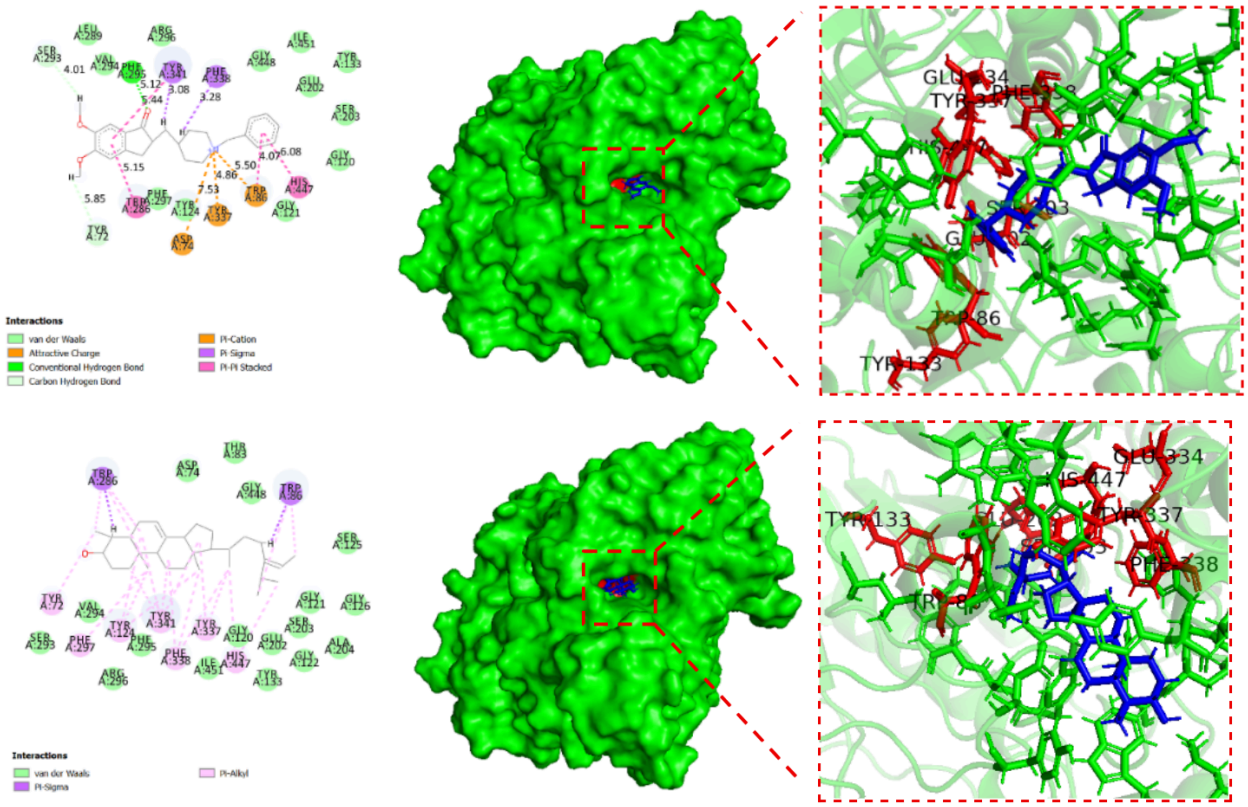

Figure 7. Visualization of 2D and 3D interactions between the natural ligand (Donepezil), the best test ligand (Citrostadienol) based on Gibbs free energy (ΔG) values, and active residues of AChE protein

DISCUSSION

An integrated interpretation was supported by the convergence of network pharmacology and molecular docking outputs. The lead candidates highlighted in this study include sterol-like molecules such as 28-isofucosterol and granisterol that show very high lipophilicity with WLOGP > 7. High lipophilicity is strongly associated with poor aqueous solubility and dissolution-limited exposure, which can reduce oral bioavailability and increase variability in pharmacokinetics (Baghel et al., 2020; Benet et al., 2016). These features also move the compounds beyond conventional Rule of Five space, where logP values > 5 are commonly linked to developability constraints, including absorption and solubility tradeoffs (Möbitz, 2024). Therefore, these highly lipophilic sterol-like leads should be interpreted as scaffold-level signals of target engagement rather than ready to advance drug candidates without mitigation.

A feasible development pathway remains possible if formulation and delivery are considered early. Lipid-based systems, such as self-nanoemulsifying drug delivery systems, can enhance oral exposure of highly lipophilic drugs by improving dispersion and apparent solubility in the gastrointestinal tract (Baloch et al., 2019). Solid lipid nanoparticles and nanostructured lipid carriers are also widely used as lipophilic colloidal carriers to improve the delivery and performance of poorly water-soluble compounds, with established formulation and characterization workflows (Akbari et al., 2022; Viegas et al., 2023). In parallel, cyclodextrin inclusion complexes can increase the solubility and stability of poorly water-soluble drugs, and hydrophilic cyclodextrin derivatives are frequently used to improve dissolution and bioavailability (Cid-Samamed et al., 2022; Nicolaescu et al., 2025).

From the union of predicted protein targets of *N. tabacum* L. bioactives and AD-associated proteins prioritized by GeneCards relevance scores, intersection analysis yielded 90 overlapping proteins. **Figure 2**

summarizes this overlap as target proteins from the intersection analysis of *N. tabacum* L. compounds and AD target proteins, indicating biologically meaningful convergence between phytochemical activity and Alzheimer's relevant pathways. Centrality-based prioritization was then applied to the protein-protein interaction network, and the hub ranking approach is consistent with common Cytoscape workflows that use topological parameters such as Degree and Betweenness to identify influential nodes in complex interactomes (Chin et al., 2014).

Enrichment results are critical to lock and biologically justify hub prioritization. **Figure 3** reports GO and KEGG pathway enrichment, and the pattern supports a three-axis rationale that integrates inflammation, kinase signaling, and cholinergic neurotransmission. The cholinergic axis is supported by enriched terms and pathways connected to acetylcholine signaling and synaptic processes, including cholinergic synapse-level biology, which is consistent with the established role of cholinergic system degeneration in cognitive decline and the clinical relevance of cholinergic modulation in AD (Klein, 2025; Rodriguez-Hernandez et al., 2024). The inflammatory axis is supported by enrichment categories that commonly map to cytokine and immune signaling, such as inflammatory response and cytokine-mediated signaling, which is coherent with the known importance of neuroinflammation and cytokine elevation, including IL-1β (Remnitz et al., 2025; Valiukas et al., 2025). The kinase axis is supported by enrichment that aligns with phosphorylation and signaling control, which fits the established mechanistic role of GSK3β in tau-related pathology and broader Alzheimer's relevant signaling regulation (Cheng et al., 2024; Zhao et al., 2024). Together, these enrichment patterns strengthen the logic of selecting IL-1β, GSK3β, and AChE as the core triad. This explicitly addresses the reviewer's concern that IL-1β and GSK3β must be represented alongside AChE in the biological narrative of the enrichment results.

Network topology and enrichment also reinforce each other at the level of mechanism. High centrality for IL-1β is consistent with the fact that microglia-driven cytokine programs and sustained inflammatory signaling can contribute to synaptic injury and neuronal vulnerability in Alzheimer's disease (Kiraly et al., 2023; Valiukas et al., 2025). GSK3β behaves as a mechanistic bridge because it is strongly linked to tau phosphorylation and is also recognized as a regulator of inflammatory balance across signaling pathways, which makes its hub status coherent with both phosphorylation-oriented enrichment and immune signaling enrichment (Kühl et al., 2024; Zhao et al., 2024). AChE remains a clinically salient node because cholinergic dysfunction is a major druggable feature of the disease, and symptomatic benefits of AChE inhibition remain supported in clinical and translational evidence (Sheikh & Ammar, 2024).

Pipeline fidelity was further supported by docking controls behaving as expected, which improves confidence in rank comparisons. Donepezil is an established AChE inhibitor used clinically in Alzheimer's disease, so its top placement and acceptable pose behavior support the validity of the AChE docking setup (Sheikh & Ammar, 2024). PF-367 is a potent and highly selective GSK3 inhibitor with evidence linked to tau phosphorylation modulation, so its expected strong performance supports the GSK3β docking baseline (Liang et al., 2016). For the *N. tabacum* L. derived ligands, **Table 4** provides the Gibbs free energy and inhibition constant results for IL-1β, GSK3β, and AChE, and **Table 3** summarizes the amino acid residues involved across target interactions, enabling residue-level interpretation rather than relying only on affinity ranks. Residue level interpretation should be connected to functional meaning, not listed as contacts alone. For AChE, interactions involving Trp86 are mechanistically important because Trp86 is a key component of the anionic subsite within the active site gorge that contributes to ligand recognition and stabilizes inhibitor binding within the aromatic gorge (Hung et al., 2025; Jaman et al., 2025; Peitzika & Pontiki, 2023). Contacts involving Ser203 further support plausible inhibition because Ser203 is part of the catalytic triad that drives

acetylcholine hydrolysis, so engagement near this catalytic machinery supports functional inhibition rather than nonproductive surface binding (Wu et al., 2026).

The ATP-binding pocket GSK3β is defined by recurrent residues involved in inhibitor binding, including Lys85, Glu97, Val135, Cys199, and Asp200, so ligand contacts at these residues are consistent with ATP-competitive kinase inhibition that is relevant to tau phosphorylation control (Alhawarri et al., 2024; Hua et al., 2023). For IL-1β, small molecule targeting is less conventional than enzyme inhibition, yet structural and experimental literature support the existence of druggable binding sites and antagonism mechanisms in IL-1β, making recurring contacts on hydrophobic patches and defined sites biologically plausible as interface modulating interactions (Hommel et al., 2023; Liu et al., 2023). **Figures 5-7** strengthen this interpretation by visualizing 2D and 3D interaction patterns for the natural ligands and the best test ligands on each target, which supports the reviewer's request to connect residue fingerprints to plausible function.

Polypharmacology should be the main framing argument because AD is multifactorial, and single-target strategies often provide limited coverage of disease biology. A single scaffold or closely related chemical family that simultaneously modulates neuroinflammation via IL-1β-linked signaling, tau-relevant kinase activity via GSK3β, and cholinergic dysfunction via AChE offers pathway-level complementarity that is difficult to achieve with one target only. This multi-target rationale aligns with modern multi-target drug design concepts in AD and supports prioritizing balanced ligands that show coherent binding and mechanistic plausibility across the three axes (Hossain & Hussain, 2025). The balanced multi-target candidates can be positioned as disease biology-aligned leads, while AChE-focused candidates can be framed as symptomatic adjuncts, consistent with current therapeutic logic where cholinesterase inhibition improves symptoms but does not fully halt disease progression (Thawabteh et al., 2024).

Finally, pharmacokinetic interpretation should explicitly connect to the presented figures and tables. **Table 1** summarizes the ADMET profile and drug-likeness metrics of *N. tabacum* L. compounds, which should be used to justify why certain candidates are prioritized for downstream testing and why others may carry solubility or exposure risks. **Figure 1** presents the BOILED Egg model interpretation. This model estimates gastrointestinal absorption and brain access from polarity and lipophilicity features and is implemented in SwissADME, supporting its use for early-stage prioritization (Daina et al., 2019; Daina & Zoete, 2016). In Alzheimer's-oriented prioritization, candidates predicted to combine favorable intestinal absorption with a higher probability of passive BBB permeation and low efflux liability are more likely to achieve meaningful brain exposure, which motivates follow-up confirmation using permeability and transporter assays alongside evaluations of solubility and metabolic stability.

CONCLUSION

Network pharmacology intersected predicted targets of *Nicotiana tabacum* L. bioactives with Alzheimer-associated proteins, yielding 90 overlapping proteins. Hub proteins were selected using centrality, where IL-1β showed Degree 37 and Betweenness 1058.7211, GSK3β showed Degree 25 and Betweenness 538.91125, and AChE showed Degree 19 and Betweenness 513.74084. Pathway prioritization was supported by enrichment, which highlighted synaptic transmission, cholinergic signaling, response to acetylcholine, and KEGG cholinergic synapse and neuroactive ligand receptor interaction, strengthening the cholinergic axis that rationalizes AChE within the triad. Leads were prioritized by three criteria: multi-target docking performance, conserved contact patterns at target sites, and ADMET limitations. Docking controls validated the workflow, and across controls plus test ligands, ΔG ranged from -6.673 to -12.275 kcal/mol, and inhibition constant ranged from 0.001 to 12.843 μM. A balanced multi-target profile supported 28 isofucosterol and granisterol as lead chemotypes, while β-amyrin and citrostadienol were retained for

GSK3β- and AChE-focused progression. Because sterol-like leads show WLOGP > 7, solubility risk and Rule of Five constraints should be mitigated using lipid-based systems or cyclodextrin-enabled formulation before further validation. Importantly, these lead chemotypes represent non-nicotine constituents of *N. tabacum* L., which supports repurposing tobacco-derived scaffolds beyond nicotine-centered narratives. Next, validation should include blood-brain barrier permeability and efflux assays, such as PAMPA BBB and MDCK MDR1, together with solubility testing under formulation-enabled conditions.

AUTHOR CONTRIBUTIONS

DRDA: Conceptualization, Methodology, Formal analysis, Investigation, Data curation, Writing – Original draft, Writing – Review and Editing. **MJW**: Software, Validation, Investigation, Data curation. **MA**: Software, Validation, Investigation. **ZA**: Software, Validation, Investigation. **MAW**: Software, Validation, Investigation. **RMP**: Conceptualization, Supervision, Project administration, Writing – Review and Editing.

ACKNOWLEDGEMENTS

The authors would like to express their sincere gratitude to Olimpiade Penelitian Siswa Indonesia (OPSI), Pusat Prestasi Nasional (PUSPRESNAS), and the Ministry of Primary and Secondary Education of the Republic of Indonesia for their support and for providing the opportunity that contributed to this research.

COMPETING INTERESTS

The authors declare that they have no known competing financial interests or personal relationships that could have appeared to influence the work reported in this paper.

FUNDING

The authors received no financial support for the research, authorship, and/or publication of this article.

ADDITIONAL INFORMATION

None.

REFERENCES

Akbari, J., Saeedi, M., Ahmadi, F., Hashemi, S. M. H., Babaei, A., Yaddollahi, S., Rostamkalaei, S. S., Asare-Addo, K., & Nokhodchi, A. (2022). Solid lipid nanoparticles and nanostructured lipid carriers: A review of the methods of manufacture and routes of administration. *Pharmaceutical Development and Technology*, *27*(5), 525–544. https://doi.org/10.1080/10837450.2022.2084554

Alhawarri, M. B., Al-Thiabat, M. G., Dubey, A., Tufail, A., Fouad, D., Alrimawi, B. H., & Dayoob, M. (2024). ADME profiling, molecular docking, DFT, and MEP analysis reveal cissamaline, cissamanine, and cissamdine from *Cissampelos capensis* L.f. as potential anti-Alzheimer's agents. *RSC Advances*, *14*(14), 9878–9891. https://doi.org/10.1039/D4RA01070A

Baghel, P., Roy, A., Verma, S., Satapathy, T., & Bahadur, S. (2020). Amelioration of lipophilic compounds in regards to bioavailability as self-emulsifying drug delivery system (SEDDS). *Future Journal of Pharmaceutical Sciences*, *6*(21). https://doi.org/10.1186/s43094-020-00042-0

Baloch, J., Sohail, M. F., Sarwar, H. S., Kiani, M. H., Khan, G. M., Jahan, S., Rafay, M., Chaudhry, M. T., Yasinzai, M., & Shahnaz, G. (2019). Self-nanoemulsifying drug delivery system (SNEDDS) for improved oral bioavailability of chlorpromazine: *In vitro* and *in vivo* evaluation. *Medicina*, *55*(5), 210. https://doi.org/10.3390/medicina55050210

Benet, L. Z., Hosey, C. M., Ursu, O., & Oprea, T. I. (2016). BDDCS, the rule of 5 and drugability. *Advanced Drug Delivery Reviews*, *101*, 89–98. https://doi.org/10.1016/j.addr.2016.05.007

Birks, J. S., & Harvey, R. J. (2018). Donepezil for dementia due to Alzheimer's disease. *Cochrane Database of Systematic Reviews*, *2018*(6). https://doi.org/10.1002/14651858.CD001190.pub3

Cantone, A. F., Burgaletto, C., Di Benedetto, G., Pannaccione, A., Secondo, A., Bellanca, C. M., Augello, E., Munafò, A., Tarro, P., Bernardini, R., & Cantarella, G. (2024). Taming microglia in Alzheimer's disease: Exploring potential implications of choline alphoscerate via α7 nAChR modulation. *Cells*, *13*(4), 309. https://doi.org/10.3390/cells13040309

Chen, Y., & Yu, Y. (2023). Tau and neuroinflammation in Alzheimer's disease: Interplay mechanisms and clinical translation. *Journal of Neuroinflammation*, *20*(1), 165. https://doi.org/10.1186/s12974-023-02853-3

Cheng, Z., Han, T., Yao, J., Wang, K., Dong, X., Yu, F., Huang, H., Han, M., Liao, Q., He, S., Lyu, W., & Li, Q. (2024). Targeting glycogen synthase kinase-3β for Alzheimer's disease: Recent advances and future prospects. *European Journal of Medicinal Chemistry*, *265*, 116065. https://doi.org/10.1016/j.ejmech.2023.116065

Chin, C.-H., Chen, S.-H., Wu, H.-H., Ho, C.-W., Ko, M.-T., & Lin, C.-Y. (2014). cytoHubba: Identifying hub objects and sub-networks from complex interactome. *BMC Systems Biology*, *8*(S4), S11. https://doi.org/10.1186/1752-0509-8-S4-S11

Cid-Samamed, A., Rakmai, J., Mejuto, J. C., Simal-Gandara, J., & Astray, G. (2022). Cyclodextrins inclusion complex: Preparation methods, analytical techniques and food industry applications. *Food Chemistry*, *384*, 132467. https://doi.org/10.1016/j.foodchem.2022.132467

Daina, A., Michielin, O., & Zoete, V. (2019). SwissTargetPrediction: Updated data and new features for efficient prediction of protein targets of small molecules. *Nucleic Acids Research*, *47*(W1), W357–W364. https://doi.org/10.1093/nar/gkz382

Daina, A., & Zoete, V. (2016). A BOILED-Egg to predict gastrointestinal absorption and brain penetration of small molecules. *ChemMedChem*, *11*(11), 1117–1121. https://doi.org/10.1002/cmdc.201600182

Hanslik, K. L., & Ulland, T. K. (2020). The role of microglia and the Nlrp3 inflammasome in Alzheimer's disease. *Frontiers in Neurology*, *11*. https://doi.org/10.3389/fneur.2020.570711

Hommel, U., Hurth, K., Rondeau, J.-M., Vulpetti, A., Ostermeier, D., Boettcher, A., Brady, J. P., Hediger, M., Lehmann, S., Koch, E., Blechschmidt, A., Yamamoto, R., Tundo Dottorello, V., Haenni-Holzinger, S., Kaiser, C., Lehr, P., Lingel, A., Mureddu, L., Schleberger, C., … Bornancin, F. (2023). Discovery of a selective and biologically active low-molecular weight antagonist of human interleukin-1β. *Nature Communications*, *14*(1), 5497. https://doi.org/10.1038/s41467-023-41190-0

Hossain, M. S., & Hussain, M. H. (2025). Multi-target drug design in Alzheimer's disease treatment: Emerging technologies, advantages, challenges, and limitations. *Pharmacology Research & Perspectives*, *13*(4). https://doi.org/10.1002/prp2.70131

Hua, L., Anjum, F., Shafie, A., Ashour, A. A., Almalki, A. A., Alqarni, A. A., Banjer, H. J., Almaghrabi, S. A., He, S., & Xu, N. (2023). Identifying promising GSK3β inhibitors for cancer management: A computational pipeline combining virtual screening and molecular dynamics simulations. *Frontiers in Chemistry*, *11*. https://doi.org/10.3389/fchem.2023.1200490

Hung, L., Sanbonmatsu, K. Y., Williams, R. F., & Chen, J. C. -H. (2025). Acetylcholinesterase: Structure, dynamics, and interactions with organophosphorus compounds. *Protein Science*, *34*(10). https://doi.org/10.1002/pro.70297

Jaman, S., Tasmi, S. F., Shahriar, I., & Halim, M. A. (2025). Histidine focused covalent inhibitors targeting acetylcholinesterase: A computational pipeline for multisite therapeutic discovery in Alzheimer's disease. *ACS Chemical Neuroscience*, *16*(20), 4025–4036. https://doi.org/10.1021/acschemneuro.5c00508

Kiraly, M., Foss, J. F., & Giordano, T. (2023). Neuroinflammation, its role in Alzheimer's disease and therapeutic strategies. *The Journal of Prevention of Alzheimer's Disease*, *10*(4), 686–698. https://doi.org/10.14283/jpad.2023.109

Klein, J. (2025). The central cholinergic synapse: A primer. *International Journal of Molecular Sciences*, *26*(19), 9670. https://doi.org/10.3390/ijms26199670

Kühl, F., Brand, K., Lichtinghagen, R., & Huber, R. (2024). GSK3-driven modulation of inflammation and tissue integrity in the animal Model. *International Journal of Molecular Sciences*, *25*(15), 8263. https://doi.org/10.3390/ijms25158263

Lauretti, E., Dincer, O., & Praticò, D. (2020). Glycogen synthase kinase-3 signaling in Alzheimer's disease. *Biochimica et Biophysica Acta (BBA) - Molecular Cell Research*, *1867*(5), 118664. https://doi.org/10.1016/j.bbamcr.2020.118664

Li, S., Ding, Q., & Wang, X. (2021). "Network target" theory and network pharmacology. In *Network Pharmacology* (pp. 1–34). Springer Singapore. https://doi.org/10.1007/978-981-16-0753-0_1

Li, Z., & Gong, C. (2025). NLRP3 inflammasome in Alzheimer's disease: Molecular mechanisms and emerging therapies. *Frontiers in Immunology*, *16*. https://doi.org/10.3389/fimmu.2025.1583886

Liang, S. H., Chen, J. M., Normandin, M. D., Chang, J. S., Chang, G. C., Taylor, C. K., Trapa, P., Plummer, M. S., Para, K. S., Conn, E. L., Lopresti-Morrow, L., Lanyon, L. F., Cook, J. M., Richter, K. E. G., Nolan, C. E., Schachter, J. B., Janat, F., Che, Y., Shanmugasundaram, V., … Vasdev, N. (2016). Discovery of a highly selective glycogen synthase kinase-3 inhibitor (PF-04802367) that modulates tau phosphorylation in the brain: Translation for PET neuroimaging. *Angewandte Chemie International Edition*, *55*(33), 9601–9605. https://doi.org/10.1002/anie.201603797

Liu, T., Chen, Y., Adil, M., Almehmadi, M., Alshabrmi, F. M., Allahyani, M., Alsaiari, A. A., Liu, P., Khan, M. R., & Peng, Q. (2023). *In silico* identification of natural product-based inhibitors targeting IL-1β/IL-1R protein–protein interface. *Molecules*, *28*(13), 4885. https://doi.org/10.3390/molecules28134885

Marucci, G., Buccioni, M., Ben, D. D., Lambertucci, C., Volpini, R., & Amenta, F. (2021). Efficacy of acetylcholinesterase inhibitors in Alzheimer's disease. *Neuropharmacology*, *190*, 108352. https://doi.org/10.1016/j.neuropharm.2020.108352

McManus, R. M., & Latz, E. (2024). NLRP3 inflammasome signalling in Alzheimer's disease. *Neuropharmacology*, *252*, 109941. https://doi.org/10.1016/j.neuropharm.2024.109941

Möbitz, H. (2024). Design principles for balancing lipophilicity and permeability in beyond rule of 5 space. *ChemMedChem*, *19*(5). https://doi.org/10.1002/cmdc.202300395

Nicolaescu, O. E., Belu, I., Mocanu, A. G., Manda, V. C., Rău, G., Pîrvu, A. S., Ionescu, C., Ciulu-Costinescu, F., Popescu, M., & Ciocîlteu, M. V. (2025). Cyclodextrins: Enhancing drug delivery, solubility and bioavailability for modern therapeutics. *Pharmaceutics*, *17*(3), 288. https://doi.org/10.3390/pharmaceutics17030288

Pan, J., Yao, Q., Wang, Y., Chang, S., Li, C., Wu, Y., Shen, J., & Yang, R. (2024). The role of PI3K signaling pathway in Alzheimer's disease. *Frontiers in Aging Neuroscience*, *16*. https://doi.org/10.3389/fnagi.2024.1459025

Peitzika, S.-C., & Pontiki, E. (2023). A review on recent approaches on molecular docking studies of novel compounds targeting acetylcholinesterase in Alzheimer disease. *Molecules*, *28*(3), 1084. https://doi.org/10.3390/molecules28031084

Pinzi, L., & Rastelli, G. (2019). Molecular docking: Shifting paradigms in drug discovery. *International Journal of Molecular Sciences*, *20*(18), 4331. https://doi.org/10.3390/ijms20184331

Remnitz, A. D., Hadad, R., Keane, R. W., Dietrich, W. D., & de Rivero Vaccari, J. P. (2025). Comparison of methods of detecting IL-1β in the blood of Alzheimer's disease subjects. *International Journal of Molecular Sciences*, *26*(2), 831. https://doi.org/10.3390/ijms26020831

Rodriguez-Hernandez, M. A., Alemany, I., Olofsson, J. K., Diaz-Galvan, P., Nemy, M., Westman, E., Barroso, J., Ferreira, D., & Cedres, N. (2024). Degeneration of the cholinergic system in individuals with subjective cognitive decline: A systematic review. *Neuroscience & Biobehavioral Reviews*, *157*, 105534. https://doi.org/10.1016/j.neubiorev.2024.105534

Sayas, C. L., & Ávila, J. (2021). GSK-3 and tau: A key duet in Alzheimer's disease. *Cells*, *10*(4), 721. https://doi.org/10.3390/cells10040721

Sheikh, M., & Ammar, M. (2024). Efficacy of 5 and 10 mg donepezil in improving cognitive function in patients with dementia: A systematic review and meta-analysis. *Frontiers in Neuroscience*, *18*. https://doi.org/10.3389/fnins.2024.1398952

Thawabteh, A. M., Ghanem, A. W., AbuMadi, S., Thaher, D., Jaghama, W., Karaman, D., & Karaman, R. (2024). Recent advances in therapeutics for the treatment of Alzheimer's disease. *Molecules*, *29*(21), 5131. https://doi.org/10.3390/molecules29215131

Valiukas, Z., Tangalakis, K., Apostolopoulos, V., & Feehan, J. (2025). Microglial activation states and their implications for Alzheimer's disease. *The Journal of Prevention of Alzheimer's Disease*, *12*(1), 100013. https://doi.org/10.1016/j.tjpad.2024.100013

Viegas, C., Patrício, A. B., Prata, J. M., Nadhman, A., Chintamaneni, P. K., & Fonte, P. (2023). Solid lipid nanoparticles vs. nanostructured lipid carriers: A comparative review. *Pharmaceutics*, *15*(6), 1593. https://doi.org/10.3390/pharmaceutics15061593

Wu, J., Wang, L., Yang, S., Pei, S., Liu, T., Zhou, Q., Huang, X., Gong, G., Wang, Q., Liu, W., & Wu, Q. (2026). In-depth analysis of acetylcholinesterase: Recent advances in structure, function and assays. *Biochemical Engineering Journal*, *226*, 109974. https://doi.org/10.1016/j.bej.2025.109974

Wu, X., Singh, S. K., Patra, B., Wang, J., Pattanaik, S., & Yuan, L. (2025). An overview of the regulation of specialized metabolism in tobacco. *Current Plant Biology*, *41*, 100431. https://doi.org/10.1016/j.cpb.2024.100431

Zhang, Wenji, Pan, X., Fu, J., Cheng, W., Lin, H., Zhang, Wenjuan, & Huang, Z. (2024). Phytochemicals derived from *Nicotiana tabacum* L. plant contribute to pharmaceutical development. *Frontiers in Pharmacology*, *15*. https://doi.org/10.3389/fphar.2024.1372456

Zhao, J., Wei, M., Guo, M., Wang, M., Niu, H., Xu, T., & Zhou, Y. (2024). GSK3: A potential target and pending issues for treatment of Alzheimer's disease. *CNS Neuroscience & Therapeutics*, *30*(7). https://doi.org/10.1111/cns.14818